

A New Noncoding RNA Arranges Bacterial Chromosome Organization

Zhong Qian,^a Mirjana Macvanin,^a Emiliós K. Dimitriadis,^b Ximiao He,^c Victor Zhurkin,^d Sankar Adhya^a

Laboratory of Molecular Biology, National Cancer Institute,^a Biomedical Engineering and Physical Science, National Institute of Biomedical Imaging and Bioengineering,^b Laboratory of Metabolism, National Cancer Institute,^c and Laboratory of Cell Biology, National Cancer Institute,^d National Institutes of Health, Bethesda, Maryland, USA

ABSTRACT Repeated extragenic palindromes (*REPs*) in the enterobacterial genomes are usually composed of individual palindromic units separated by linker sequences. A total of 355 annotated *REPs* are distributed along the *Escherichia coli* genome. RNA sequence (RNAseq) analysis showed that almost 80% of the *REPs* in *E. coli* are transcribed. The DNA sequence of *REP*₃₂₅ showed that it is a cluster of six repeats, each with two palindromic units capable of forming cruciform structures in supercoiled DNA. Here, we report that components of the *REP*₃₂₅ element and at least one of its RNA products play a role in bacterial nucleoid DNA condensation. These RNA not only are present in the purified nucleoid but bind to the bacterial nucleoid-associated HU protein as revealed by RNA IP followed by microarray analysis (RIP-Chip) assays. Deletion of *REP*₃₂₅ resulted in a dramatic increase of the nucleoid size as observed using transmission electron microscopy (TEM), and expression of one of the *REP*₃₂₅ RNAs, nucleoid-associated noncoding RNA 4 (naRNA4), from a plasmid restored the wild-type condensed structure. Independently, chromosome conformation capture (3C) analysis demonstrated physical connections among various *REP* elements around the chromosome. These connections are dependent in some way upon the presence of HU and the *REP*₃₂₅ element; deletion of HU genes and/or the *REP*₃₂₅ element removed the connections. Finally, naRNA4 together with HU condensed DNA *in vitro* by connecting *REP*₃₂₅ or other DNA sequences that contain cruciform structures in a pairwise manner as observed by atomic force microscopy (AFM). On the basis of our results, we propose molecular models to explain connections of remote cruciform structures mediated by HU and naRNA4.

IMPORTANCE Nucleoid organization in bacteria is being studied extensively, and several models have been proposed. However, the molecular nature of the structural organization is not well understood. Here we characterized the role of a novel nucleoid-associated noncoding RNA, naRNA4, in nucleoid structures both *in vivo* and *in vitro*. We propose models to explain how naRNA4 together with nucleoid-associated protein HU connects remote DNA elements for nucleoid condensation. We present the first evidence of a noncoding RNA together with a nucleoid-associated protein directly condensing nucleoid DNA.

Received 8 July 2015 Accepted 3 August 2015 Published 25 August 2015

Citation Qian Z, Macvanin M, Dimitriadis EK, He X, Zhurkin V, Adhya S. 2015. A new noncoding RNA arranges bacterial chromosome organization. *mBio* 6(4):e00998-15. doi:10.1128/mBio.00998-15.

Editor Bonnie Bassler, Princeton University

Copyright © 2015 Qian et al. This is an open-access article distributed under the terms of the [Creative Commons Attribution-Noncommercial-ShareAlike 3.0 Unported license](https://creativecommons.org/licenses/by-nc-sa/4.0/), which permits unrestricted noncommercial use, distribution, and reproduction in any medium, provided the original author and source are credited.

Address correspondence to Sankar Adhya, sadhya@helix.nih.gov.

This article is a direct contribution from a Fellow of the American Academy of Microbiology.

Noncoding RNAs (ncRNAs) present in both prokaryotic and eukaryotic cells do not function as mRNA, tRNA, or rRNA (1). Although many ncRNAs of different sizes and different functions have been widely reported (2–6), new ncRNAs with new functions are still being discovered. Recently, we discovered a novel ncRNA, transcribed from a specific repeated extragenic palindromic element, *REP*₃₂₅, in the chromosome of *Escherichia coli* by RNA IP followed by microarray analysis (RIP-Chip) assays of the nucleoid-associated HU protein (7). In this paper, we termed it as nucleoid-associated ncRNA (naRNA). *REP* elements in the enterobacterial genomes, first reported 30 years ago, contain individual palindromes separated by linkers (8–10). The functions of the *REPs* have been speculated to be related to transcription termination signals, binding sites for proteins, cleavage sites for DNA gyrase, and, possibly, manipulation of nucleoid structures (11–14). In this study, we investigated potential functions of the *REP*₃₂₅ element, which is located between genes *yjdB* (*phnA*) and *yjdB* (*phnB*), and its RNA products. *REP*₃₂₅ contains six homolo-

gous units (Fig. 1A). Each repeat is composed of two palindromic cruciform-generating motifs, *Y* and *Z*₂, connected by a short linker, *l*. Cells deleted for the *REP*₃₂₅ segment and/or *hup* genes encoding the nucleoid-associated HU protein showed a decondensed nucleoid structure, suggesting that these two factors participate in nucleoid condensation (7). RNA sequencing (RNAseq) analysis and nucleoid RNA tiling array clearly showed the existence of RNA species transcribed from each unit of *REP*₃₂₅, named naRNA1 to naRNA6 (Fig. 1A). Multialignment of DNA sequences of the 6 repeats in *REP*₃₂₅ showed high homology (Fig. 1B). Each naRNA contains two potential hairpins, corresponding to *Y* and *Z*₂ motifs (Fig. 1C). It is unknown whether these six RNAs are transcribed independently or are the result of processing of a larger RNA transcribed from a common promoter (the promoter of the upstream gene, *yjdB*). One of these RNAs is naRNA4, which binds two dimeric forms of HU, HU $\alpha\alpha$ and HU $\alpha\beta$. In this report, we show that the expression of naRNA4 from a plasmid restores the decondensed morphology of the nucleoid caused by

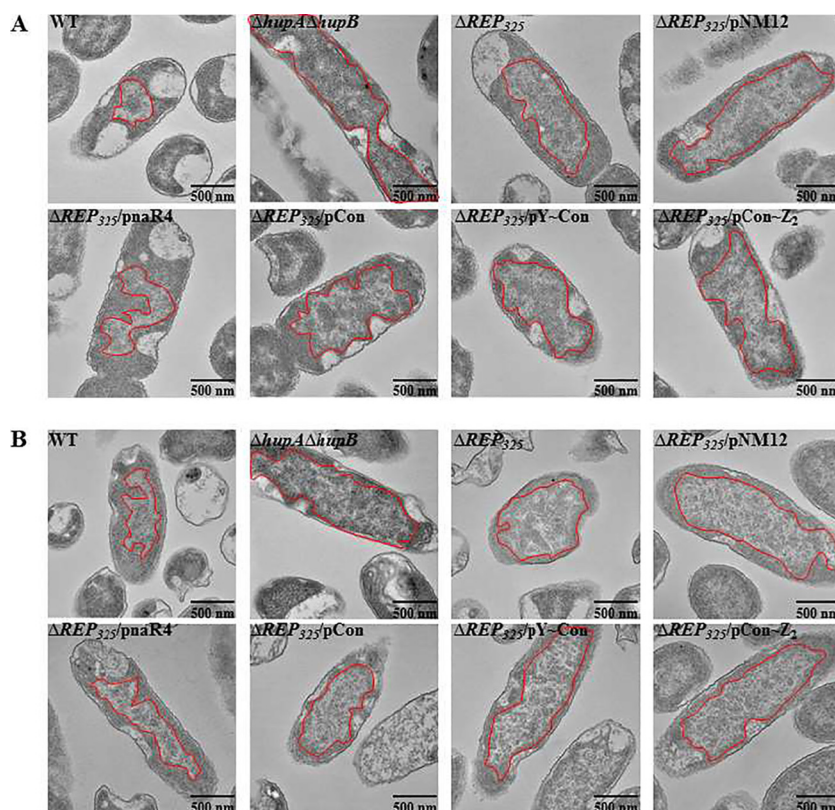


FIG 2 TEM analysis of nucleoid morphology of cells in log phase (A) or stationary phase (B). *E. coli* MG1655 is used as the wild-type (WT) strain. Deletions of HU genes were constructed by replacement of *hupA* and *hupB* by ampicillin (Amp) and chloramphenicol (Cm) antibiotic cassettes. The ΔREP_{325} mutant was constructed by replacement of the wild-type allele by a sac-Cat cassette. The construction of the plasmids is described in Materials and Methods. The plasmids were transformed into the ΔREP_{325} strain, resulting in the following mutant strains: the $\Delta REP_{325}/pNM12$ mutant, the $\Delta REP_{325}/pnaR4$ mutant, the $\Delta REP_{325}/pconRNA$ mutant, the $\Delta REP_{325}/pYRNA$ mutant, and the $\Delta REP_{325}/pZ_2RNA$ mutant. Nucleoids are identified in the EM pictures by red outlines. Scale bars, 500 nm. The apparent differences in cell sizes are the result of angular variations that occurred during cell slicing. Only representative TEM images are shown.

contain the Y and Z_2 potential hairpins. The typical structure of naRNA4 is shown in Fig. 1C.

Decondensation of nucleoid *in vivo*: TEM analysis. Transmission electron microscopy (TEM) observations previously showed that deletion mutants of HU genes ($\Delta hupA \Delta hupB$ strain) and/or of the REP_{325} element (ΔREP_{325} gene strain) decondensed the *E. coli* nucleoid in both growing and nongrowing cells compared to a compacted nucleoid observed in the wild-type strain under similar conditions, suggesting that HU and part or all of REP_{325} DNA and/or its RNA product affect nucleoid architecture (7). We extended the TEM observations further by investigating the details of REP_{325} participation in the nucleoid structure. We first confirmed that in growing cells, compared to wild-type results, deletion of HU genes or of REP_{325} decondensed the nucleoid size (Fig. 2A; nucleoids are outlined in red). Moreover, the REP_{325} deletion strain carrying a plasmid vector showed no change in decondensed nucleoid morphology. But expression of naRNA4 from the plasmid reproducibly condensed the nucleoid. We observed some overcondensation that was most likely due to overexpression of naRNA4. The expression of an unrelated RNA from the same plasmid had no effect on the decondensed nucleoid. We also tested the effect of expression of derivatives of naRNA4 containing only a Z_2 or Y motif in the same REP_{325} -deleted cells. The expression of RNA containing only the Z_2 or Y motif alone, unlike that of the intact naRNA4, did not restore the nucleoid morphol-

ogy to wild type, although we do not know anything about the relative stability of naRNA4 or its truncated derivatives under the conditions of the experiments. TEM analysis performed with non-growing cells in the same set of strains gave identical results; only the presence of an intact naRNA4 caused nucleoid condensation (Fig. 2B). We note that, in the absence of any simple way to quantify the nucleoid volume in TEM observations, we estimated the size of the nucleoid in two-dimensional (2-D) analysis of the thin sections (shown by red outlines in Fig. 2). Although these observations show the involvement of HU and naRNA4 in nucleoid condensation, a direct participation of any part of the REP_{325} element in the process is not apparent. If DNA is involved in the condensation, as seems very likely, other DNA sequences homologous to REP_{325} may fulfill the same role. In summary, this is first demonstration of a direct involvement of an ncRNA in DNA condensation at the molecular level.

Intersegmental chromosomal interactions *in vivo*: 3C analysis. We hypothesized that one plausible mechanism of nucleoid structural organization is that of facilitating contacts between REP elements around the chromosome by naRNA4 and the nucleoid protein HU. To test the idea, we employed the chromosome conformation capture (3C) approach, the use of which has been established in studies of distal intrachromosomal interactions *in vivo* in both eukaryotes and prokaryotes (18–20). We designed primers for 23 randomly selected REP segments, including

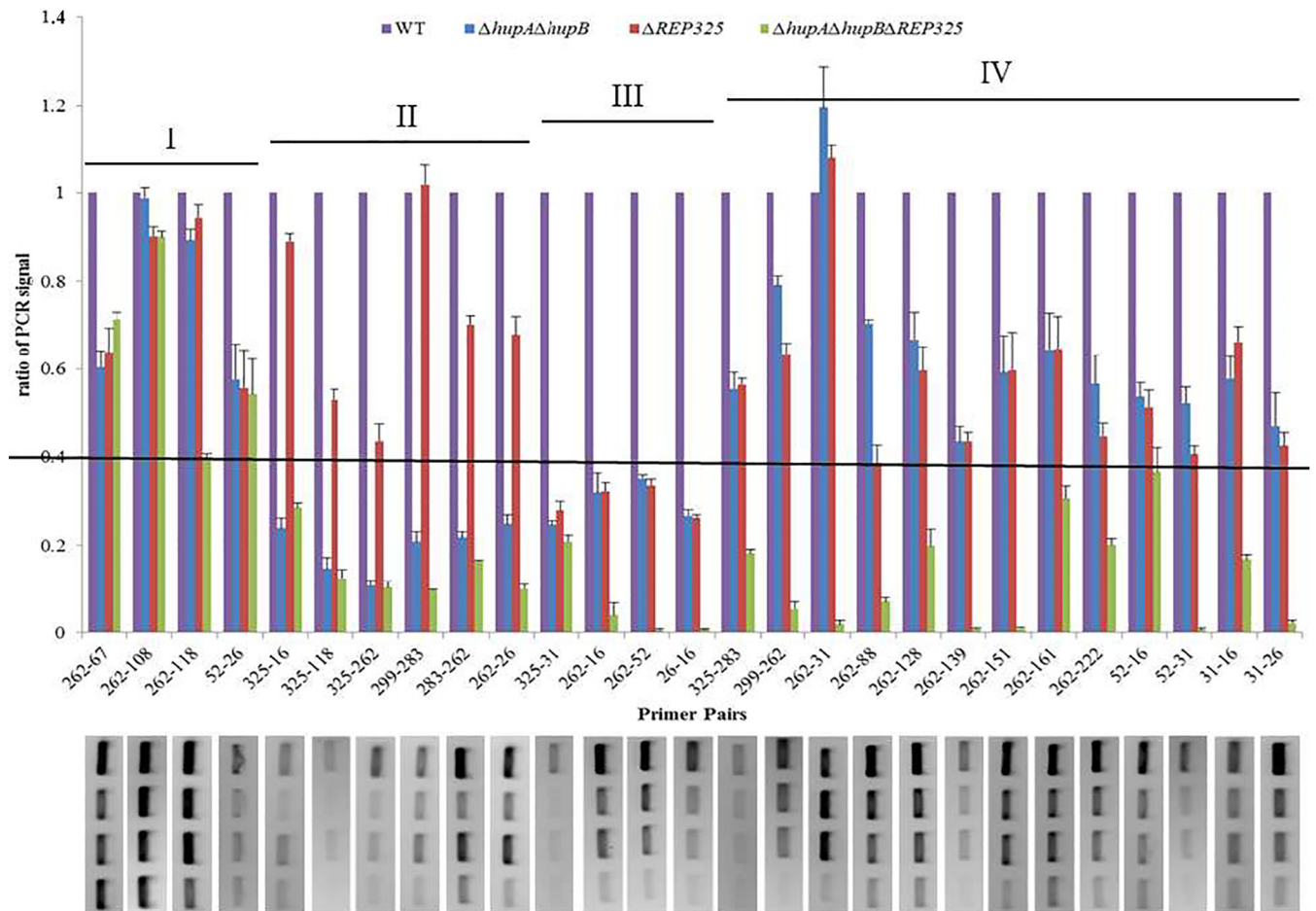


FIG 3 3C analysis of the wild-type, $\Delta hupA \Delta hupB$ mutant, ΔREP_{325} mutant, and $\Delta hupA \Delta hupB \Delta REP_{325}$ mutant strains. (Top panel) Graphic presentation of 3C x -axis data showing the combinations of designated primers (see Table S1 in the supplemental material). y -axis data show the ratios of PCR signals in mutant strains to those in the wild-type strain. A ratio change of 0.4 (horizontal solid black line) or lower is considered significant. Error bars indicate standard deviations (STDEV) ($n = 4$ sets of independent experiments). 3C data were grouped into four classes: (I) HU and naRNA4 independent, (II) HU dependent, (III) HU and naRNA4 dependent, and (IV) HU or naRNA4 dependent. (Bottom panel) Typical PCR bands on 2% agarose gel. From top to bottom, the bands are amplified from 3C samples of the wild-type, $\Delta hupA \Delta hupB$, ΔREP_{325} , and $\Delta hupA \Delta hupB \Delta REP_{325}$ strains. As indicated at the top of the upper panel, the corresponding color codes are as follows: wild-type strain, purple; $\Delta hupA \Delta hupB$ strain, blue; ΔREP_{325} strain, red; $\Delta hupA \Delta hupB \Delta REP_{325}$ strain, green.

REP_{325} , around the chromosome to investigate potential connections between REP sites (primer sequences are listed in Table S1 in the supplemental material). Of 253 pairs tested, 27 combinations showed positive PCR amplifications, suggesting that the corresponding DNA segments may be connected to each other (Fig. 3). These pairs were further tested by 3C in the following mutants: the Δhup mutant, the ΔREP_{325} mutant, and $\Delta hup \Delta REP_{325}$ mutant. We measured the ratio of PCR signals in each mutant compared to that in the wild-type strain after normalization to an internal control. In interpreting the positive amplification results in 3C experiments in the following discussion, we assume that an observed contact involves the REP elements and not another DNA sequence present nearby in the chromosome. Similarly, when a contact signal observed in the wild-type strain is missing in the ΔREP_{325} deletion strain, we assume that it is because of the absence of naRNA4. The effect of the HU and REP_{325} deletions on the observed intrachromosomal interactions were grouped into four classes. (i) HU and naRNA4 independent. Deletion of either HU and/or REP_{325} has no effect on the interactions suggesting perhaps

other NAPs and RNAs are involved in DNA contacts (4 out of 27). (ii) HU dependent. Deletion of the HU gene significantly affected the interactions while deletion of REP_{325} did not (6 out of 27). In these cases, HU together with other RNA may be involved in bringing DNA contacts. (iii) HU and naRNA4 dependent. Deletion of either the HU gene or REP_{325} significantly affected the interactions (4 out of 27). In these cases, both HU and naRNA4 are specifically involved in DNA contacts. (iv) HU or naRNA4 dependent. Only deletion of both HU and REP_{325} significantly affected the interactions while removal of either HU or RNA4 did not (13 out of 27). In this group, HU collaborates with another RNA or naRNA4 collaborates with another protein for DNA-DNA interactions.

DNA condensation mediated by HU and naRNA4 *in vitro*: AFM analysis. Both TEM and 3C analyses showed the involvement of HU and naRNA4 in nucleoid organization. However, they did not reveal any mechanistic details. We used AFM to monitor any condensing effects of HU protein and naRNA4 on naked supercoiled DNA *in vitro* to get some insights about the mecha-

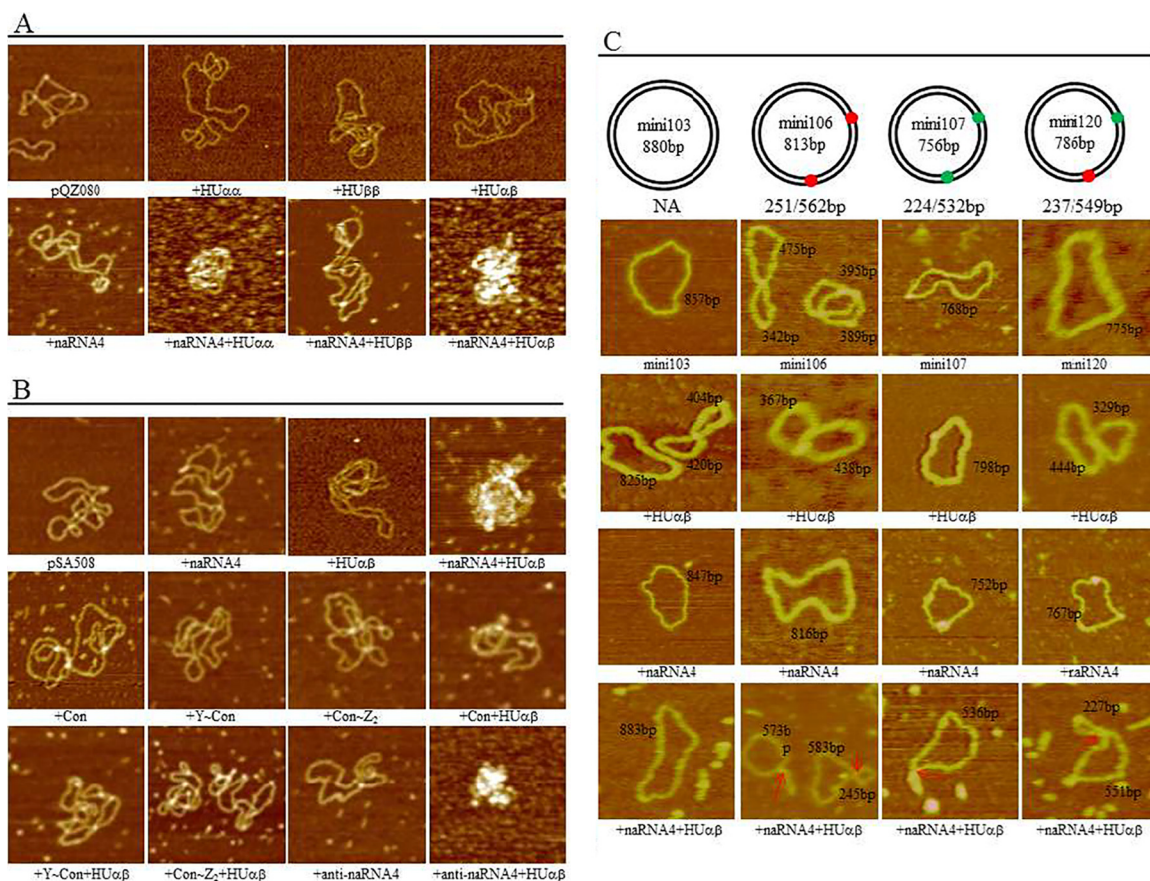


FIG 4 AFM images of plasmid DNA with HU and naRNA4. The components added for reactions are indicated below each AFM image. (A) AFM images of large-plasmid DNA containing the cloned *REP*₃₂₅ element (pQZ080) in the original pSA508 plasmid vector (19) in the presence of different HU and naRNA4 molecules. (B) AFM images of the DNA vector plasmid (pSA508) without the *REP*₃₂₅ clone in the presence and absence of HU and naRNA4. (C) Minicircle DNA. (Top panel) Schematic representation of each minicircle DNA used. A red dot indicates the insertion site of one *REP*₃₂₅ repeat; a green dot indicates the *rhoC* transcription terminator that contains a palindrome. Both of the DNA elements are proven binding sites of HU (21). The lengths of expected sizes of the DNA loops are shown below each DNA molecule representation. (Bottom panel) AFM images of minicircle DNA in different combinations of HU and naRNA4. A red arrow indicates the looping complex. Only representative AFM images are shown.

nism(s) of their action. A plasmid containing one *REP*₃₂₅ (pQZ080) was used as the template for AFM (Fig. 4). The addition of naRNA4 or of different HU dimers to the plasmid did not noticeably change its supercoiled morphology. The absence of any effect of HU in this experiment is consistent with previous reports (15, 21). However, the presence of either HU $\alpha\alpha$ or HU $\alpha\beta$ together with naRNA4 dramatically condensed the DNA, apparently because of the presence of multiple intersegmental contacts, thus demonstrating that naRNA4 collaborates with HU in condensing DNA (Fig. 4A). Note that either HU $\alpha\alpha$ or HU $\alpha\beta$ dimer works but not HU $\beta\beta$ dimer ($\alpha\alpha$, $\alpha\beta$, and $\beta\beta$). Since the plasmid DNA contained only one *REP*₃₂₅ element, the multiple contacts very likely involve either nonspecific DNA binding or some other sequences in the plasmid that allow DNA contacts. The *REP*₃₂₅ palindromic repeats generate cruciform structures in a supercoiled state. We believe that several transcription terminators (22) that are present in the plasmid and which also generate cruciform structures perform the role of *REP*₃₂₅. Consistent with this idea, the addition of HU and naRNA4 to the parental plasmid (pSA508) containing no authentic *REP* element but several transcription terminators also resulted in DNA condensation (Fig. 4B). To investigate the features of naRNA4 required in DNA condensation,

we first tested whether an intact naRNA4 is needed to condense DNA. We performed AFM analysis with three 77-nucleotide (nt) RNAs: a nonspecific control RNA, an RNA containing only the Y motif, and an RNA containing only the Z₂ motif (see Table S2 in the supplemental material). Compared to naRNA4, none of these RNAs condensed DNA (Fig. 4B), which is in agreement with the TEM data (Fig. 2). We also asked whether the exact sequences or only hairpin features of Z₂ and Y motifs are involved. We synthesized a 77-nt-long RNA whose sequence was the exact complement of naRNA4. This anti-naRNA4 molecule has an RNA sequence completely different from that of naRNA4 but should contain two hairpin structures. Figure 4B shows that the anti-naRNA4 also condensed DNA in the presence of HU protein, indicating that it is the secondary structure of naRNA4 and not the sequence of the RNA itself that is important in DNA condensation.

Because of the large sizes of pQZ080 and pSA508 (3.9 kb and 3.5 kb, respectively), we could not discern the precise organization of the DNA contact points involved in the observed DNA condensation. To simplify the condensed DNA structure, we tested a number of minicircle DNAs which contain 0, 1, or 2 potential condensation sites (cruciform structures originated from *REP*₃₂₅

or one of the transcription terminators, *rpoC*, present in the parental plasmid, pSA508) at marked positions: mini103, mini104, mini105, mini106, mini107, and mini120 (Fig. 4C; see also Fig. S2 in the supplemental material). Any looping generated using the marked cruciform sites can be discerned by measuring the size of the DNA loops between contact points. As elaborated below, consistent with our proposal, HU- and RNA4-mediated DNA condensation *in vitro* requires only a cruciform structure in DNA and not other parts of the multipalindromic unit and the presence of both HU and naRNA4 on minicircle DNAs (Fig. 4C). “Figure 8” structures, which are caused by either random crossover of DNA or specific bridging of DNA due to the presence of HU and naRNA4, were observed in all minicircle DNAs. To determine whether the looping was random or specific, we measured each loop from the figure 8 structures in the minicircle DNAs in the presence of naRNA4 and HU protein. We observed that the frequency of figure 8 structures with the expected loop sizes resulting from interactions between any two marked cruciform structures was significantly higher in all minicircle DNAs except in mini103, which has no cruciform structure. For example, we found 79 figure 8 structures in mini103 in the presence of naRNA4 and HU, and none was found with an expected loop size. In mini106, mini107, and mini120 containing two cruciforms, the ratios of the numbers of observed figure 8 structures with expected loop sizes to the total numbers of counted structures were 24/49, 48/101, and 28/53, respectively. These results suggest that HU and naRNA4 form bridges between two cruciforms present in a minicircle DNA.

For mini104 and mini105 plasmids, which contain one *rpoC* transcription terminator of *pSA508* and one *REP*₃₂₅ repeat, respectively, we observed only random figure 8 structures and, occasionally, two or more minicircle DNAs bridged together by a complex core (red arrows in Fig. S2 in the supplemental material), suggesting that two cruciform structures present in different DNA molecules can connect.

DISCUSSION

It has become clear that the organization of the chromosome in *E. coli* is not random. The chromosome is not merely a disordered aggregate of randomly coiled DNA. Instead, it is a dynamic but spatially organized defined entity that undergoes strictly controlled and reproducible changes when they are needed (23). Structural models of elements such as “macro domains,” “supercoiled topological loops,” “filaments,” and “remote connections” are suggested to represent structural constituents of chromosomes from observations using different approaches (19, 24–27). A number of NAPs, such as the HU, Fis, IHF, H-NS, and SMC proteins, modulate chromosome structure. We focused on HU, which binds to DNA nonspecifically but prefers distorted DNA structures such as nicks, gaps, bends, and cruciforms (28, 29). Due to its high abundance and growth-phase-dependent subunit compositions (HU $\alpha\alpha$, HU $\alpha\beta$, and HU $\beta\beta$), HU is believed to modulate chromosome structure in accordance with the growth phase of the cell (30). We confirmed that HU binds to naRNA4 and to several other RNAs by electrophoretic mobility shift assay (EMSA) (see Fig. S3 in the supplemental material), but not all HU-RNA bindings could help DNA condensation both *in vivo* (Fig. 2) and *in vitro* but bound to those which contained two hairpin structures (Fig. 4). Thus, an HU-naRNA4 interaction may be somewhat unusual and specific; the presence of at least two

hairpin motifs, such as Z₂ and Y, in the RNA is needed for DNA condensation. We conclude that two cruciform structures in DNA, not yet completely defined, interact with each other in a pairwise fashion for DNA condensation, which needs both HU and naRNA4. We propose four mechanisms for interactions between two DNA cruciforms mediated by HU and naRNA4 (Fig. 5). (i) For DNA-naRNA-HU-naRNA-DNA interactions, each cruciform structure binds to one hairpin of naRNA and two DNA-bound RNAs are bridged together by an HU dimer using the other hairpins of the two naRNAs (Fig. 5A). (ii) For DNA-naRNA(HU)-DNA interactions, the model is similar to model i, but the stoichiometry of HU and naRNA in the complex is 1:1. HU binding to naRNA makes the latter amenable to interaction with two cruciforms (Fig. 5B). (iii) For DNA-HU-naRNA-HU-DNA interactions, HU binds to cruciform DNA; two bound-HU dimers are then connected by a molecule of naRNA through the two hairpins (Fig. 5C). (iv) For DNA-HU(naRNA)-DNA interactions, the model is similar to model iii, but the stoichiometry of HU and naRNA in the complex is 1:1. naRNA binding to HU makes the latter potent for interactions with two cruciform structures. We note here that in models ii and iv, it is possible that the roles of naRNA and HU, respectively, could be only catalytic and that they are not involved in the complex. At this stage, we are unable to prefer one model to the others except that a specific interaction between HU and a DNA cruciform structure has been previously established (31, 32), which would support models iii and iv. Cross-linking of the condensed DNA complexes followed by fragmentation and chemical identification of the products may distinguish between the different models.

MATERIALS AND METHODS

Construction of strains and plasmids. Wild-type *E. coli* MG1655 and the $\Delta hupA \Delta hupB$ mutant were previously described (7). The ΔREP ₃₂₅ strain was constructed by mini- λ recombinering, in which *REP*₃₂₅ was replaced by a Cat-SacB cassette (33, 34). Plasmid pQZ080 was constructed with the insertion of *REP*₃₂₅ into pSA508 (35) at SacI to BamHI sites. Minicircle DNA was purified according to the method of Choy and Adhya (35). Plasmid pNM12 was from Nadim Majdalani (NIH, USA). DNA fragments encoding the naRNA4 gene and Con, Y-Con, and Con-Z₂ genes were amplified using chemically synthesized single-stranded DNAs (ssDNAs) as templates and inserted into pNM12 at MscI to HindIII sites. All recombinant plasmids and pNM12 were transformed into the ΔREP ₃₂₅ strain.

Validation of expression of *REP*₃₂₅ by analysis of RNAseq data. Raw RNAseq data for *E. coli* MG1655 obtained from the NCBI Sequence Read Archive (accession no. SRP006793) (17) were mapped onto the *E. coli* genome using Novoalign software and allowing up to two mismatches between a 36-nt read and the genome sequence. Two different strategies, using unique map reads and total map reads, were applied, and the unique map read results and total map read results were preserved separately, with multiple alignments of up to 50 different locations in the genome. The alignment files (sorted by bam format) were used for visualization in tracks in the genome browser at the University of Southern California, Santa Cruz (UCSC) (36).

Synthesis of RNA used in AFM analysis. A series of complementary ssDNAs that contain a T7 promoter sequence (5'-TAATACGACTCACT ATAGGGAGA-3') followed by experimental sequences and their complements, listed in Table S2 in the supplemental material, were chemically synthesized. The double-stranded DNAs (dsDNAs) were obtained by annealing the appropriate complementary ssDNAs (7). Synthesis and purification of RNAs were completed by the use of an AmpliScribe T7-Flash transcription kit according to the manufacturer's instructions (Epicentre, Madison, WI). The quality and quantity of RNAs were determined by the

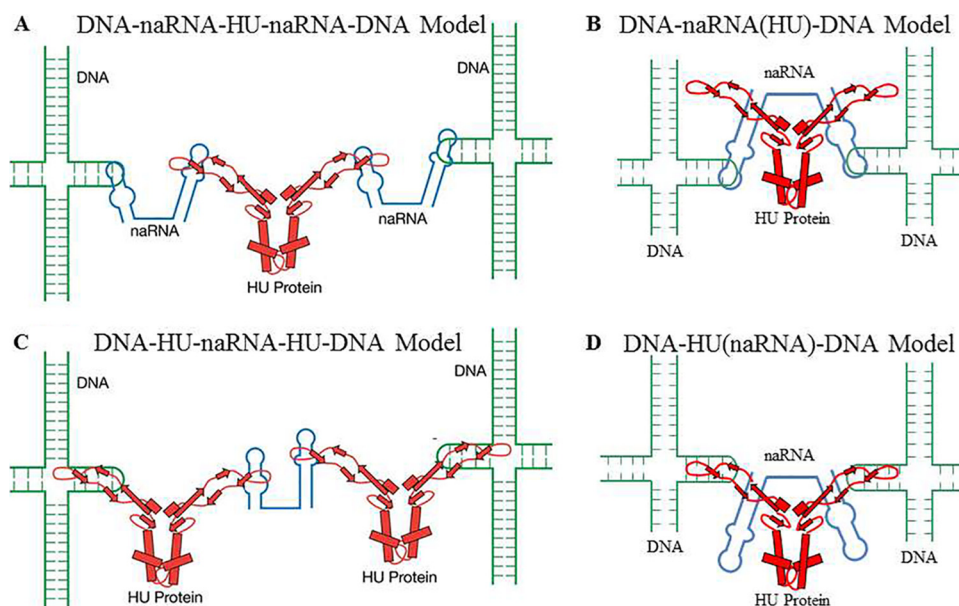


FIG 5 Models of HU- and naRNA-mediated DNA condensation. (A) DNA-naRNA-HU-naRNA-DNA model. Cruciform DNA structures connect with a hairpin in naRNA. Two DNA-bound RNAs are then bridged together by an HU dimer. (B) DNA-naRNA(HU)-DNA data are presented similarly to the model data presented in panel A, but the stoichiometry of HU and naRNA in the complex is 1:1. HU facilitates the binding of an RNA molecule to two cruciform structures. (C) DNA-HU-naRNA-HU-DNA:HU binds to cruciform DNA structures; two bound-HU dimers are then connected by a molecule of naRNA. How naRNA interacts with DNA cruciform, if such an interaction occurs, is unknown, but HU interaction with cruciform-generating DNA has been established (31, 32). (D) DNA-HU(naRNA)-DNA data are presented similarly to the model data presented in panel C, but the stoichiometry of HU and naRNA is 1:1. naRNA binding to HU facilitates one molecule of HU binding to two DNA cruciform structures.

use of an agarose gel and a NanoDrop spectrophotometer (Thermo Scientific, Wilmington, DE), respectively. For RNAs used in the gel shift assay, [α - 32 P]UTP was used instead of the unlabeled UTP provided in the kit.

Electrophoretic mobility shift assay. Electrophoretic mobility shift assays in gels were done as described before (37, 38) with modifications. Radioactively labeled RNAs were incubated with increasing amounts (0 to 1.6 mM) of HU protein in binding buffer containing 20 mM Tris-HCl (pH 7.5), 0.2 M NaCl, and 10% glycerol at 37°C for 20 min. The mixtures were separated by the use of 8% prerun native polyacrylamide gels and 1× Tris-borate-EDTA (TBE) buffer. Gels were finally exposed to X-film at -80°C.

TEM analysis of nucleoid structure in *E. coli*. Strains used in TEM analysis were inoculated from plates with appropriate antibiotics into M63 minimal medium with 0.2% fructose, 0.05% Casamino Acids, and proper antibiotics and incubated at 37°C overnight. The cultures were diluted into fresh medium as mentioned above with 0.1% arabinose and grown to log or stationary phase for harvest. One milliliter of fresh cultures was mixed with an equal volume of Fixation buffer (8% formaldehyde–4% glutaraldehyde–0.2 M cacodylate buffer or 2× phosphate-buffered saline [PBS]) and kept at room temperature for 2 h. The fixed cell solutions were stored at 4°C until TEM analyses were performed. Cells were spun down to form a small pellet and then processed for EM analysis of thin sections. Briefly, the pellet was postfixated in 1% osmium tetroxide (Electron Microscopy Sciences, Ft. Washington, PA)–0.1 M cacodylate buffer for 1 h at room temperature, stained in 0.5% uranyl acetate–0.1 M acetate buffer for 1 h, and then dehydrated in a series of ethanol (35%, 50%, 75%, 95%, and 100%) and propylene oxide (100%) solutions. The pellets were infiltrated into 100% propylene oxide and epoxy resin (1:1) overnight and embedded in pure resin the following day. The epoxy resin was cured in a 55°C oven for 48 h, and 70-to-80-nm-thick sections were made and mounted on copper grids (300 mesh) and stained using uranyl acetate followed by lead citrate. The cells were examined and imaged using a model H7600 TEM (Hitachi, Tokyo, Japan) operated at 80 kV. Images

were captured by a bottom-mounted charge-coupled-device (CCD) camera (Gatan, Pleasanton, CA).

3C analysis of intrachromosomal interactions. 3C analysis was carried out as previously described (19). Primers are listed in Table S1 in the supplemental material. After PCR, the products were separated by electrophoresis on a 2% agarose gel. Each amplified band of the images was quantitatively measured by the use of 1-D gel analysis software (UVP Bioimaging Systems). The fold change of interaction frequency for each primer pair was determined as the ratio of the 3C products of a given mutant to those of the wild-type strain after normalization to the internal control. Each frequency value represents the average of the results of four independent experiments.

AFM analysis of DNA condensation *in vitro*. Sample preparations and AFM analysis were performed as reported previously (19) with some modifications. After the binding step, samples were not directly delivered to AFM analysis. Formaldehyde was added to reach a final concentration of 1%, and the reaction mixture was incubated for 15 min at room temperature, followed by quenching with glycine at a final concentration of 0.125 M for 5 min at room temperature.

Images were preprocessed using the instrument image processing software and then exported for further analysis with the NIH ImageJ image processing software package. The lengths of DNA loops observed in minicircle DNA were measured by tracing.

SUPPLEMENTAL MATERIAL

Supplemental material for this article may be found at <http://mbio.asm.org/lookup/suppl/doi:10.1128/mBio.00998-15/-/DCSupplemental>.

Text S1, DOC file, 0.1 MB.
Text S2, XLSX file, 0.04 MB.
Text S3, XLSX file, 0.02 MB.
Text S4, XLSX file, 0.02 MB.
Figure S1, PDF file, 0.2 MB.
Figure S2, PDF file, 0.1 MB.
Figure S3, PDF file, 0.05 MB.

Table S1, PDF file, 0.05 MB.

Table S2, PDF file, 0.05 MB.

ACKNOWLEDGMENTS

This research was supported by the Intramural Research Program of the National Institutes of Health, National Cancer Institute, Center for Cancer Research.

We thank our colleagues Dale Lewis, Amlan Dhar, Phuoc Le, Sangmi Lee, and Andrei Trostel for assistance.

REFERENCES

- Hüttenhofer A, Vogel J. 2006. Experimental approaches to identify non-coding RNAs. *Nucleic Acids Res* 34:635–646. <http://dx.doi.org/10.1093/nar/gkj469>.
- Gripenland J, Netterling S, Loh E, Tiensuu T, Toledo-Arana A, Johansson J. 2010. RNAs: regulators of bacterial virulence. *Nat Rev Microbiol* 8:857–866. <http://dx.doi.org/10.1038/nrmicro2457>.
- Han BW, Chen YQ. 2013. Potential pathological and functional links between Long noncoding RNAs and hematopoiesis. *Sci Signal* 6. <http://dx.doi.org/10.1016/j.ijmm.2013.04.002>.
- Hoe CH, Raabe CA, Rozhdetsvensky TS, Tang TH. 2013. Bacterial sRNAs: regulation in stress. *Int J Med Microbiol* 303:217–229. <http://dx.doi.org/10.1016/j.ijmm.2013.04.002>.
- Tomizawa J, Som T. 1984. Control of ColE1 plasmid replication: enhancement of binding of RNA I to the primer transcript by the Rom protein. *Cell* 38:871–878. [http://dx.doi.org/10.1016/0092-8674\(84\)90282-4](http://dx.doi.org/10.1016/0092-8674(84)90282-4).
- Battesti A, Majdalani N, Gottesman S. 2011. The RpoS-mediated general stress response in *Escherichia coli*. *Annu Rev Microbiol* 65:189–213. <http://dx.doi.org/10.1146/annurev-micro-090110-102946>.
- Macvanin M, Edgar R, Cui F, Trostel A, Zhurkin V, Adhya S. 2012. Noncoding RNAs binding to the nucleoid protein HU in *Escherichia coli*. *J Bacteriol* 194:6046–6055. <http://dx.doi.org/10.1128/JB.00961-12>.
- Gilson E, Saurin W, Perrin D, Bachellier S, Hofnung M. 1991. The BIME family of bacterial highly repetitive sequences. *Res Microbiol* 142:217–222. [http://dx.doi.org/10.1016/0923-2508\(91\)90033-7](http://dx.doi.org/10.1016/0923-2508(91)90033-7).
- Gilson E, Saurin W, Perrin D, Bachellier S, Hofnung M. 1991. Palindromic units are part of a new bacterial interspersed mosaic element (BIME). *Nucleic Acids Res* 19:1375–1383. <http://dx.doi.org/10.1093/nar/19.7.1375>.
- Gilson E, Clément JM, Brutlag D, Hofnung M. 1984. A family of dispersed repetitive extragenic palindromic DNA sequences in *E. coli*. *EMBO J* 3:1417–1421.
- Boccard F, Prentki P. 1993. Specific interaction of IHF with RIBs, a class of bacterial repetitive DNA elements located at the 3' end of transcription units. *EMBO J* 12:5019–5027.
- Espéli O, Boccard F. 1997. In vivo cleavage of *Escherichia coli* BIME-2 repeats by DNA gyrase: genetic characterization of the target and identification of the cut site. *Mol Microbiol* 26:767–777. <http://dx.doi.org/10.1046/j.1365-2958.1997.6121983.x>.
- Espéli O, Moulin L, Boccard F. 2001. Transcription attenuation associated with bacterial repetitive extragenic BIME elements. *J Mol Biol* 314:375–386. <http://dx.doi.org/10.1006/jmbi.2001.5150>.
- Gilson E, Perrin D, Hofnung M. 1990. DNA polymerase I and a protein complex bind specifically to *E. coli* palindromic unit highly repetitive DNA: implications for bacterial chromosome organization. *Nucleic Acids Res* 18:3941–3952. <http://dx.doi.org/10.1093/nar/18.13.3941>.
- Ohniwa RL, Muchaku H, Saito S, Wada C, Morikawa K. 2013. Atomic force microscopy analysis of the role of major DNA-binding proteins in organization of the nucleoid in *Escherichia coli*. *PLoS One* 8:e72954. <http://dx.doi.org/10.1371/journal.pone.0072954>.
- Pettijohn DE, Hecht R. 1974. RNA molecules bound to the folded bacterial genome stabilize DNA folds and segregate domains of supercoiling. *Cold Spring Harb Symp Quant Biol* 38:31–41. <http://dx.doi.org/10.1101/SQB.1974.038.01.006>.
- Raghavan R, Groisman EA, Ochman H. 2011. Genome-wide detection of novel regulatory RNAs in *E. coli*. *Genome Res* 21:1487–1497. <http://dx.doi.org/10.1101/gr.119370.110>.
- Dekker J, Rippe K, Dekker M, Kleckner N. 2002. Capturing chromosome conformation. *Science* 295:1306–1311. <http://dx.doi.org/10.1126/science.1067799>.
- Qian Z, Dimitriadis EK, Edgar R, Eswaramoorthy P, Adhya S. 2012. Galactose repressor mediated intersegmental chromosomal connections in *Escherichia coli*. *Proc Natl Acad Sci U S A* 109:11336–11341. <http://dx.doi.org/10.1073/pnas.1208595109>.
- Umbarger MA, Toro E, Wright MA, Porreca GJ, Baù D, Hong SH, Fero MJ, Zhu LJ, Marti-Renom MA, McAdams HH, Shapiro L, Dekker J, Church GM. 2011. The three-dimensional architecture of a bacterial genome and its alteration by genetic perturbation. *Mol Cell* 44:252–264. <http://dx.doi.org/10.1016/j.molcel.2011.09.010>.
- Balandina A, Kamashev D, Rouviere-Yaniv J. 2002. The bacterial histone-like protein HU specifically recognizes similar structures in all nucleic acids. DNA, RNA, and their hybrids. *J Biol Chem* 277:27622–27628. <http://dx.doi.org/10.1074/jbc.M201978200>.
- Lewis DE, Adhya S. 2002. In vitro repression of the gal promoters by GalR and HU depends on the proper helical phasing of the two operators. *J Biol Chem* 277:2498–2504. <http://dx.doi.org/10.1074/jbc.M108456200>.
- Robinow C, Kellenberger E. 1994. The bacterial nucleoid revisited. *Microbiol Rev* 58:211–232.
- Deng S, Stein RA, Higgins NP. 2005. Organization of supercoil domains and their reorganization by transcription. *Mol Microbiol* 57:1511–1521. <http://dx.doi.org/10.1111/j.1365-2958.2005.04796.x>.
- Espeli O, Mercier R, Boccard F. 2008. DNA dynamics vary according to macromolecular topography in the *E. coli* chromosome. *Mol Microbiol* 68:1418–1427. <http://dx.doi.org/10.1111/j.1365-2958.2008.06239.x>.
- Wiggins PA, Cheveralls KC, Martin JS, Lintner R, Kondev J. 2010. Strong intranucleoid interactions organize the *Escherichia coli* chromosome into a nucleoid filament. *Proc Natl Acad Sci U S A* 107:4991–4995. <http://dx.doi.org/10.1073/pnas.0912062107>.
- Wang W, Li GW, Chen C, Xie XS, Zhuang X. 2011. Chromosome organization by a nucleoid-associated protein in live bacteria. *Science* 333:1445–1449. <http://dx.doi.org/10.1126/science.1204697>.
- Castaigne B, Zelwer C, Laval J, Boiteux S. 1995. HU protein of *Escherichia coli* binds specifically to DNA that contains single-strand breaks or gaps. *J Biol Chem* 270:10291–10296. <http://dx.doi.org/10.1074/jbc.270.17.10291>.
- Kamashev D, Balandina A, Rouviere-Yaniv J. 1999. The binding motif recognized by HU on both nicked and cruciform DNA. *EMBO J* 18:5434–5444. <http://dx.doi.org/10.1093/emboj/18.19.5434>.
- Claret L, Rouviere-Yaniv J. 1997. Variation in HU composition during growth of *Escherichia coli*: the heterodimer is required for long term survival. *J Mol Biol* 273:93–104. <http://dx.doi.org/10.1006/jmbi.1997.1310>.
- Aki T, Adhya S. 1997. Repressor induced site-specific binding of HU for transcriptional regulation. *EMBO J* 16:3666–3674. <http://dx.doi.org/10.1093/emboj/16.12.3666>.
- Vitoc CI, Mukerji I. 2011. HU binding to a DNA four-way junction probed by forster resonance energy transfer. *Biochemistry* 50:1432–1441. <http://dx.doi.org/10.1021/bi1007589>.
- Lee EC, Yu D, Martinez de Velasco J, Tassarollo L, Swing DA, Court DL, Jenkins NA, Copeland NG. 2001. A highly efficient *Escherichia coli*-based chromosome engineering system adapted for recombinogenic targeting and subcloning of BAC DNA. *Genomics* 73:56–65. <http://dx.doi.org/10.1006/geno.2000.6451>.
- Court DL, Swaminathan S, Yu D, Wilson H, Baker T, Bubunenko M, Sawitzke J, Sharan SK. 2003. Mini-lambda: a tractable system for chromosome and BAC engineering. *Gene* 315:63–69. [http://dx.doi.org/10.1016/S0378-1119\(03\)00728-5](http://dx.doi.org/10.1016/S0378-1119(03)00728-5).
- Choy HE, Adhya S. 1993. RNA polymerase idling and clearance in gal promoters: use of supercoiled minicircle DNA template made in vivo. *Proc Natl Acad Sci U S A* 90:472–476. <http://dx.doi.org/10.1073/pnas.90.2.472>.
- Raney BJ, Dreszer TR, Barber GP, Clawson H, Fujita PA, Wang T, Nguyen N, Paten B, Zweig AS, Karolchik D, Kent WJ. 2013. Track data hubs enable visualization of user-defined genome-wide annotations on the UCSC genome browser. *Bioinformatics* 30:1003–1005.
- Qian Z, Meng B, Wang Q, Wang Z, Zhou C, Tu S, Lin L, Ma Y, Liu S. 2009. Systematic characterization of a novel gal operon in *Thermoanaerobacter tengcongensis*. *Microbiology* 155:1717–1725. <http://dx.doi.org/10.1099/mic.0.025536-0>.
- Qian Z, Wang Q, Tong W, Zhou C, Liu S. 2010. Regulation of galactose metabolism through the HisK:GalR two-component system in *Thermoanaerobacter tengcongensis*. *J Bacteriol* 192:4311–4316. <http://dx.doi.org/10.1128/JB.00402-10>.